Structural Studies of Metal Binding by Inositol Monophosphatase: Evidence for Two-Metal Ion Catalysis†

Roger Bone,*,‡ Lori Frank,‡ James P. Springer,‡ and John R. Atack‖

Department of Biophysical Chemistry, Merck Research Laboratories, P.O. Box 2000, Rahway, New Jersey 07065, and Department of Biochemistry, Merck Research Laboratories, Neurosciences Research Center, Terlings Park, Eastwick Road, Harlow, Essex CM20 2QR, U.K.

Received January 21, 1994; Revised Manuscript Received May 11, 1994®

ABSTRACT: The structure of inositol monophosphatase has been determined to 2.60 Å resolution in complexes with Mn^{2+} and with Mn^{2+} and phosphate. In the Mn^{2+} complex, three metal cations and one Cl^- were bound in the active site on each of the two subunits of the enzyme. Ligands to the three metals include the side chains of Glu 70, Asp 90, Asp 93, and Asp 220, the carbonyl group of Ile 92, several solvent molecules, and the chloride, which is a ligand to each of the cations. When phosphate is soaked into these Mn^{2+} cocrystals, one of the three Mn^{2+} ions is expelled from the active site, leaving metal ions with octahedral and tetrahedral coordination geometry. In addition, the structure of apoinositol monophosphatase was determined to 2.5 Å resolution. Residues 70–75, a two-turn helical segment which is involved in metal coordination, moves away from the metal binding site by 2–3 Å in the absence of cations. Residues 30–40, which wrap around the metal binding site and interact with the metal indirectly through solvent molecules and protein ligands to the metal, become disordered in the absence of metal. In various metal complexes, segmental mobility is also observed in the residues which form the metal binding sites. The results of these studies of the interaction of inositol monophosphatase with cations suggest that the enzyme accomplishes phosphate ester hydrolysis using two metal ions, one with octahedral and one with tetrahedral coordination geometry. Broad metal-binding specificity appears to result from extensive flexibility in several of the protein segments which contribute metal ligands, from the presence of alternate metal ligands and from metal coordination spheres which include water molecules.

Inositol monophosphatase (EC 3.1.3.25) catalyzes the hydrolysis of inositol monophosphates produced both in the *de novo* biosynthesis of inositol from glucose 6-phosphate and in the recovery of inositol from inositol phosphates formed during phosphatidylinositol-mediated signal transduction (Berridge & Irvine, 1989; Berridge *et al.*, 1982, 1989; Sherman *et al.*, 1986; Hallcher & Sherman, 1980; Majerus *et al.*, 1988). On the basis of the role of the phosphatase in the phosphatidylinositol signaling pathway and the observation that the enzyme is inhibited uncompetitively by Li^+, it has been suggested as the molecular site of action of Li^+ therapy for manic-depressive illness (Hallcher & Sherman, 1980; Berridge & Irvine, 1989). The enzyme is a dimer of 30 kDa subunits (277 residues) which requires Mg^{2+} as a cofactor (Gee *et al.*, 1988; McAllister *et al.*, 1992). Activation by Mg^{2+} shows positive cooperativity which has been attributed to interactions between the phosphatase subunits (Ganzhorn & Chanal, 1990; Leech *et al.*, 1993). At high concentrations, Mg^{2+} inhibits the enzyme (Hallcher & Sherman, 1980) and appears to interact with the same site as Li^+ (Ganzhorn & Chanal, 1990; Leech *et al.*, 1993). Selectivity for Mg^{2+} is poor: Zn^{2+} and Mn^{2+} support partial activity, while many divalent and trivalent cations are inhibitory (Hallcher & Sherman, 1980; Takimoto *et al.*, 1985; Pollack *et al.*, 1993, 1994).

Recently the structures of complexes of human inositol monophosphatase with inhibitory Gd^{3+} and either D-Ins(1)P,[1] L-Ins(1)P, or sulfate have been determined to resolutions of 2.3, 2.2, and 2.1 Å (Bone *et al.*, 1992, preceding paper in this issue). On the basis of these structures, it was proposed that nucleophilic attack on phosphorus is accomplished by a metal-bound water that is activated by hydrogen-bonding interactions with residues Glu 70 and Thr 95. In addition, it appeared that expulsion of the ester oxygen was promoted by three aspartate residues acting together (Asp 90, Asp 93, and Asp 220), either to donate a proton to the leaving group or to form another metal binding site from which a second Mg^{2+} coordinates to the ester oxygen during the transition state (Bone *et al.*, preceding paper in this issue). Direct observation of metal binding to the second site would be prevented if Li^+ from the crystallization solvent (3–4 M Li^+; Bone *et al.*, 1992) was bound at this site because Li^+ has just two electrons and is virtually invisible in an X-ray crystallography experiment.

Experiments in which residues that appeared to be involved in metal binding were mutated support the proposal that residues Glu 70, Asp 90, Asp 93, and Thr 95 are involved in metal binding and/or catalysis (Pollack *et al.*, 1993). However, the results of these experiments are consistent with either of the two mechanisms which have been proposed to explain how the enzyme facilitates ester leaving. Furthermore, these experiments have led to the suggestion that Glu 70 may not be a metal ligand when Mg^{2+} is bound by the enzyme. To establish whether a second metal binding site exists, whether

† The final refined coordinates have been deposited in the Protein Data Bank (entry names: 1IMC, 1IMD, and 1IMF).

* Author to whom correspondence should be addressed. Present address: 3-Dimensional Pharmaceuticals, 3700 Market St., Philadelphia, PA 19104.

‡ Department of Biophysical Chemistry.

‖ Department of Biochemistry.

® Abstract published in *Advance ACS Abstracts,* July 15, 1994.

[1] Abbreviations: D-Ins(1)P, D-*myo*-inositol 1-phosphate; L-Ins(1)P, L-*myo*-inositol 1-phosphate; Ins(1)P, *myo*-inositol 1-phosphate; EDTA, ethylenediaminetetraacetic acid; EGTA, ethylenebis(oxyethylenenitrilo)-tetraacetic acid; Tris, tris(hydroxymethyl)aminomethane; rms, root mean square.

0006-2960/94/0433-9468$04.50/0

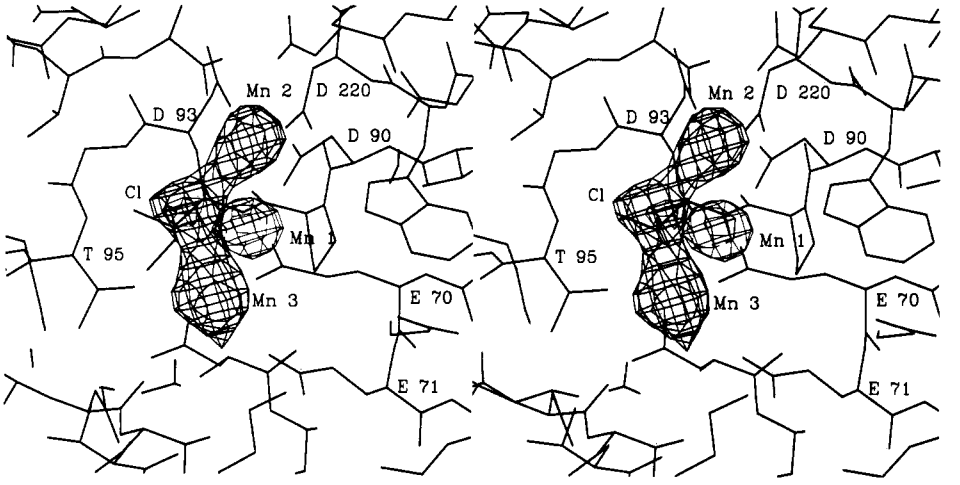

FIGURE 1: Stereodrawing of a difference electron density map of the active site region of the A subunit of the inositol monophosphatase complex with Mn^{2+} and Cl^-. Structure factors and phases were calculated as described in the text. The locations of three Mn^{2+} binding sites and the Cl^- binding site are identified. The map is contoured at 3 times the rms value of the map. No negative contours were observed at this contour value.

or not Glu 70 is a metal ligand when divalent cations are bound by the enzyme, and what the coordination geometry of the metal binding site(s) might be, the structures of inositol monophosphatase complexes with Mn^{2+} and with Mn^{2+} and phosphate have been determined. Furthermore, to increase our understanding of the metal-binding specificity of the enzyme, we have determined the structure of inositol monophosphatase in the absence of metals (apoenzyme). Suprisingly, the results of these studies show that there are three metal binding sites on each subunit of the enzyme and suggest that the enzyme catalyzes phosphate ester hydrolysis using two metal ions. Poor metal-binding selectivity appears to be a consequence of flexibility in one of the metal binding sites and the presence of several solvent molecules in the coordination sphere of the metal.

EXPERIMENTAL PROCEDURES

Materials. Cloned human inositol monophosphatase was purified from *Escherichia coli* as previously described (Diehl *et al.*, 1990; McAllister *et al.*, 1992) and crystallized by vapor diffusion (Felhammer & Bode, 1975). Mn^{2+} and inositol monophosphatase cocrystals were grown by combining 2 μL of well buffer containing 10% poly(ethylene glycol) 8000 (EM Science; average molecular weight 7000–9000), 5 mM glutathione, 5 mM $MnCl_2$, 3 mM NaN_3, and 50 mM 4-morpholinepropanesulfonic acid (adjusted to pH 7.5) with 2 μL of protein solution containing 1 mM EGTA, 2 mM *o*-phenanthroline, 20 mM Tris, and 10–15 mg/mL phosphatase. Crystals of the enzyme complex with phosphate and Mn^{2+} were prepared by adding an equal volume of 40 mM potassium phosphate (pH 7.4) in well buffer to a vapor diffusion drop containing an enzyme and Mn^{2+} cocrystal. Crystals of inositol monophosphatase with no ligands bound were obtained by combining 2 μL of well buffer containing 25% poly(ethylene glycol) 4000 (BDH; average molecular weight 3600–4400), 3 mM glutathione, and 3 mM NaN_3 with 2 μL of protein solution. Crystals appeared after approximately 1 month of equilibration, and the mother liquor had a pH value of 4.5 when tested with pH test strips (MCB). Isomorphous crystals were grown at a slightly higher pH value (5.0) by combining 3 μL of well buffer containing 20% poly(ethylene glycol) 8000 (EM Science; average molecular weight 7000–9000), 7.5 mM glutathione, 5 mM sodium phosphate, 1.5 mM $MgSO_4$, and 3 mM NaN_3 with 2 μL of protein solution.

Data Collection. Data were collected and processed using monochromatic Cu Kα X-rays and a Rigaku automated X-ray imaging system for the phosphatase complex with Mn^{2+} alone and with Mn^{2+} and phosphate. Data were collected from single crystals of the apoenzyme using a Siemens multiwire X-ray area detector and processed using version 2.0 of the Xengen software (Howard *et al.*, 1987).

Mn^{2+} Complex Structure Determination. Crystals of the complex of inositol monophosphatase with Mn^{2+} which had been grown from poly(ethylene glycol) solutions appeared identical to crystals of the Gd^{3+} complex grown from Li_2SO_4 solutions. In addition, the crystals were in the same space group and had cell dimensions within 1% of the cell dimensions of crystals of the phosphatase complex with Gd^{3+} and sulfate (Bone *et al.*, 1992). Starting from the structure of the phosphatase complex with Gd^{3+} minus all solvent and ligands (initial crystallographic R = 0.44), XPLOR (Brunger *et al.*, 1987) was used to refine an overall temperature factor and to carry out rigid body refinement of the position and orientation of each subunit. After refinement of the atomic positions using XPLOR (Brunger *et al.*, 1987), difference electron density maps were calculated to determine whether Mn^{2+} was bound at the active site (Figure 1). Three metal ions were clearly present along with what appeared to be a chloride ion. After the three Mn^{2+} cations and chloride had been placed in each active site, the structure was refined using a simulated annealing protocol (Brunger *et al.*, 1990) and then several iterations of manual model adjustment (Sack, 1988), refinement of atomic positions, and refinement of individual temperature factors were done. Distances between Mn^{2+} and ligands were not constrained explicitly during refinement. The C-terminus of subunit A was considerably more disordered than in the Gd^{3+} complex, and residues 271–277 were omitted from the model in addition to the N-terminal three residues of both subunits and the C-terminal residue of subunit B. Disordered side chains were assigned occupancy values of 0.0. Final rms bond and angle deviations and the final crystallographic R-value are shown in Table 1 along with the cell dimensions and data reduction statistics.

Mn^{2+} and Phosphate Complex. Crystals of the complex between inositol monophosphatase, Mn^{2+}, and phosphate were isomorphous with the Mn^{2+} cocrystals (Table 1). Starting from the structure of the phosphatase complex with Mn^{2+} minus all solvent but including the Mn^{2+} ions filling sites 1 and 2 (initial crystallographic R = 0.32), XPLOR (Brunger

Table 1: Statistics for Structure Determinations

parameter	crystal			
metal	none	none	Mn^{2+}	Mn^{2+} and PO_4
precipitant	PEG 4000	PEG 8000	PEG 8000	PEG 8000
pH	4.5	5.0	7.5	7.4
space group	$P3_121$	$P3_121$	$P3_221$	$P3_221$
cell edges (Å)	$a = b = 100.75$, $c = 62.12$	$a = b = 100.83$ $c = 62.51$	$a = b = 85.20$, $c = 152.33$	$a = b = 85.85$, $c = 153.60$
resolution (Å)	10.0–2.7	8.0–2.5	8.0–2.6	8.0–2.6
R_{merge}[a]	0.069	0.053	0.078	0.083
completeness (%)	98.4	97.4	95.0	95.0
$I > 2\sigma_I$	66	64	70	70
refinement	PROLSQ	PROLSQ/ XPLOR	XPLOR	XPLOR
R_{cryst}[b]	0.25	0.177	0.185	0.188
rms bond dev (Å)	0.017	0.016	0.010	0.010
rms angle dev (°)		3.3	1.25	1.25

[a] $R_{merge} = (\Sigma\Sigma|I_j(h) - \langle I(h)\rangle|/(\Sigma\Sigma I_j(h))$; summations done over all reflections from a crystal. [b] $R_{cryst} = (\Sigma||F_{obs}| - |F_{calc}||)/(\Sigma|F_{obs}|)$.

et al., 1987) was used to carry out rigid body refinement of the position and orientation of each subunit. After refinement of the atomic positions using XPLOR (Brunger *et al.*, 1987), difference electron density maps were calculated and phosphate was placed into the difference electron density. Several iterations of manual model adjustment (Sack, 1988), refinement of atomic positions, and refinement of individual temperature factors were done, and refinement statistics are shown in Table 1. Distances between Mn^{2+} and ligands were not constrained during refinement.

Apoenzyme Structure Determination. Precession photography and intensity data indicated that crystals of inositol monophosphatase grown in the absence of any ligands were in space group $P3_221$ or $P3_121$ with cell edges $a = b = 100.75$ Å and $c = 62.12$ Å. On the basis of the unit cell volume (Mathews, 1968) and an assumption that the solvent content was near 50%, the asymmetric unit of the crystal appeared to be a phosphatase monomer (30 kDa). One subunit of the structure of the inositol monophosphatase complex with Gd^{3+} was used as a model for molecular replacement calculations using the MERLOT suite of programs (Fitzgerald, 1988). The rotation function calculation (Crowther, 1972), using data between 8 and 4 Å resolution with $I/\sigma_I > 3.0$, produced a map in which there was one clear peak at Euler angles $\alpha = 56.67°$, $\beta = 54.00°$, and $\gamma = 180.0°$ with a peak height 8.7 times the rms value of the map (next peak at 4.7 times the rms map value). Translation function calculations (Crowther & Blow, 1967) were done using the same resolution range for both possible space groups. These calculations yielded single peaks with heights in the range of 10.5–12.5 times the rms map value and produced consistent solutions for x, y, and z ($x = 0.52$, $y = 0.84$, $z = 0.445$) only for the space group $P3_121$. Rigid body refinement (Ward *et al.*, 1975) of the entire model using data between 8.0 and 2.7 Å reduced the crystallographic R-value from 0.439 to 0.38. CORELS rigid body refinement (Sussman, 1985) of individual residues and ϕ, ψ, and χ angles was followed by cycles of restrained refinement of atomic positions using PROLSQ (Hendrickson, 1985) and manual rebuilding of the model (Jones, 1978) and produced a crystallographic R-value of 0.25 with an rms bond deviation of 0.017 Å.

Data extending to higher resolution were obtained from an isomorphous crystal which had been grown from PEG in the presence of 1.5 mM Mg^{2+} and 5.0 mM phosphate at pH 5.0. Difference electron density maps indicated that neither metal nor phosphate were present in the metal binding site, and it was concluded that the structures were the same. The absence of both Mg^{2+} and phosphate was not surprising because of the low pH and the presence of chelating agents in excess of the Mg^{2+} concentration. Refinement of the structure of the apoenzyme was continued using the data from the PEG crystal grown at higher pH which extended to 2.5 Å resolution, and the final stages of restrained refinement were completed using XPLOR (Brunger *et al.*, 1987; Table 1). Throughout the refinement process, residues 30–40 were absent and not included in the protein model. N-terminal sequence analysis of redissolved crystals indicated that only the normal N-terminus of the protein was present (D. Boulton, unpublished results) and provided no evidence that any proteolysis of the polypeptide chain had occurred in the region of residues 30–40. On the basis of these observations, it was concluded that residues 30–40 extend into a nearby solvent channel where they are disordered. In addition, three N-terminal residues and the C-terminal residue were disordered.

RESULTS

Mn^{2+} Complex. The structure of cocrystals of inositol monophosphatase and Mn^{2+} grown from poly(ethylene glycol) clearly reveals the presence of three Mn^{2+} binding sites and a chloride binding site on each subunit of the phosphatase dimer (Figure 1). The three Mn^{2+} binding sites on each subunit have been identified on the basis of the close proximity of large peaks in the difference electron density maps to oxygen atoms and the previous identification of one of the sites as a cation binding site (Bone *et al.*, 1992). Mn^{2+} binding site 1 is located 2.1–2.3 Å from the carboxylates of Glu 70 and Asp 90 and the carbonyl of Ile 92 and had previously been identified as the Gd^{3+} binding site (Table 2). Mn^{2+} binding site 2 is located 2.1–2.4 Å from the carboxylates of Asp 90, Asp 93, and Asp 220 and had been predicted on the basis of phosphatase complexes with substrates (Bone *et al.*, preceding paper in this issue; Table 2). Surprisingly, a third Mn^{2+} binding site (site 3) was observed at a distance of approximately 2.4 Å from Glu 70. In addition, there appears to be one water ligand to site 1 and three water ligands to site 3, with each of the water ligands also forming hydrogen bonds to the protein. The chloride binding site has been identified on the basis of the proximity of this site to each of the Mn^{2+} sites (2.7–2.8 Å; Table 2) and the inability of other known components of the crystallization buffer to fit the difference electron density. Possible anionic contaminants such as sulfate were excluded because they could not be placed in the Cl^- electron density without having inappropriately close contacts with one of the Mn^{2+} cations. After refinement, temperature factors for the chloride and Mn^{2+} ions Mn1, Mn2, and Mn3 were 29, 24, 36, and 31 $Å^2$ for subunit A and 29, 22, 34, and 38 $Å^2$ for subunit B. These values are consistent with the identifications of the electron density peaks as Cl^- and Mn^{2+} ions.

The distance between the chloride and Mn^{2+} ions is 2.7–2.8 Å and is approximately the sum of the ionic radii of the two

Table 2: Metal–Ligand Distances

		interatomic distances between metal ions and ligands (Å)					
		Mn^{2+}		Mn^{2+} and PO_4		Gd^{3+} [a]	
		subunit		subunit		subunit	
site	ligand	A	B	A	B	A	B
1	Glu 70 OE2	2.12	2.07	2.25	2.09	2.43	2.57
	Asp 90 OD1	2.26	2.26	2.19	2.23	2.34	2.42
	Asp 90 OD2					2.92	2.99
	Ile 92 O	2.14	2.12	2.03	2.11	2.56	2.32
	Thr 95 OG1					2.73	2.87
	W1	2.08	2.06	1.97	2.03	2.61	2.63
	W2					2.59	2.62
	Cl^-	2.71	2.76				
	SO_4/PO_4 O2			2.30	2.26	2.58	2.59
	SO_4/PO_4 O3			2.55	2.44	2.71	2.86
2	Asp 90 OD2	2.35	2.22	2.39	2.38		
	Asp 93 OD2	2.27	2.13	2.25	2.30		
	Asp 220 OD2	2.13	2.17	2.17	2.17		
	Cl^-	2.58	2.82				
	PO_4 O2			2.14	2.20		
3	Glu 70 OE1	2.57	2.31				
	W3	2.11	2.13				
	W4	2.09	2.02				
	W5	2.11	2.05				

[a] Values from Bone *et al.* (1992).

ions (1.7 Å for Cl^- and 0.9 Å for Mn^{2+}; Huheey, 1978). Although no other ligands to the chloride are observed, the anion is located at the positive end of the dipole of the two-turn α helix that spans residues 95–100. The lengths of coordinate bonds between oxygen atoms and the cations (2.1–2.4 Å) are consistent with values expected for Mn^{2+} coordination (~2.2 Å; Carrell, 1988). Mn^{2+} ions Mn1 and Mn3 appear to have five ligands in distorted geometries which are either trigonal bipyramids or square pyramids. It can not be ruled out that additional water ligands for these metal ions are present but not observed. The Mn^{2+} ion filling site 2 appears to have four ligands in a slightly distorted tetrahedral geometry. Although the coordination geometry of site 2 is more clearly defined, the geometry of each of the site appears to be distorted by the Cl^- anion.

Metal binding site 2 is positioned well to interact with the ester oxygen of the substrate during the transition state for ester hydrolysis. Superposition of the structures of the phosphatase complex with Mn^{2+} and the phosphatase complex with D-Ins(1)P and Gd^{3+} (Bone *et al.*, preceding paper in this issue) reveals that the Mn^{2+} in site 2 would be located 2.22 Å from the ester oxygen of the substrate and 2.25 Å from the nonbridging phosphate oxygen which is coordinated to the metal in binding site 1 (Figure 2). Slight adjustments in the substrate position and/or the positions of the three Asp residues which form metal binding site 2 would allow the coordination geometry of metal 2 to be tetrahedral with either the ester oxygen or the nonbridging phosphate oxygen as a metal ligand or trigonal bipyramidal with both atoms as ligands. Mn^{2+} is bound in site 1 in the same location as the Gd^{3+} in substrate complexes with the enzyme and retains the same protein ligands. Mn^{2+} ion 3 is bound only 1.7 Å from the position occupied by the water nucleophile (W2) in substrate complexes with the enzyme and appears to have displaced this water molecule. One of the phosphoryl oxygens from the substrate would be able to coordinate to the third Mn^{2+} (O–Mn^{2+} distance = 2.25 Å) while maintaining the other intermolecular interactions that stabilize the substrate complex.

Phosphatase Complex with Mn^{2+} and PO_4. An initial difference electron density map ($|F_{O1}| - |F_{O2}|$) of the inositol monophosphatase complex with Mn^{2+} and phosphate was made using structure factors from the Mn^{2+} cocrystal (F_{O1}), structure factors from the phosphate-soaked Mn^{2+} cocrystal (F_{O2}), and phases calculated from the final refined model of the Mn^{2+} complex with inositol monophosphatase. This map clearly indicated that phosphate soaking led to expulsion of the third Mn^{2+} ion from the active site on each subunit (Figure 3). Mn^{2+} binding site 1, which had previously been identified as the Gd^{3+} binding site (Bone *et al.*, 1992), is retained and located 2.1–2.3 Å from the carboxylates of Glu 70 and Asp 90 and the carbonyl of Ile 92 (Table 2). Mn^{2+} binding site 2 is also retained and located 2.1–2.4 Å from the carboxylates of Asp90, Asp 93, and Asp 220. Initial difference electron density maps did not have strong positive or negative features near the Cl^-, suggesting that phosphate was directly superimposed on the chloride position. However, when difference electron density maps were calculated after the structure had been refined with Cl^- rather than phosphate in the model, positive electron density appeared near the phosphate oxygens opposite from the metal ions.

After refinement, the phosphate is located with oxygen O2 2.1–2.3 Å from both remaining Mn^{2+} ions, oxygen O3 2.5 Å from Mn^{2+} site 1, oxygen O1 3.3 Å from Mn^{2+} site 2, and oxygen O4 within hydrogen-bonding distance of the amide groups of residues 94 and 95 (Table 2, Figures 4 and 5). The coordination geometry of metal binding site 1 appears to be octahedral, while the geometry of site 2 appears tetrahedral.

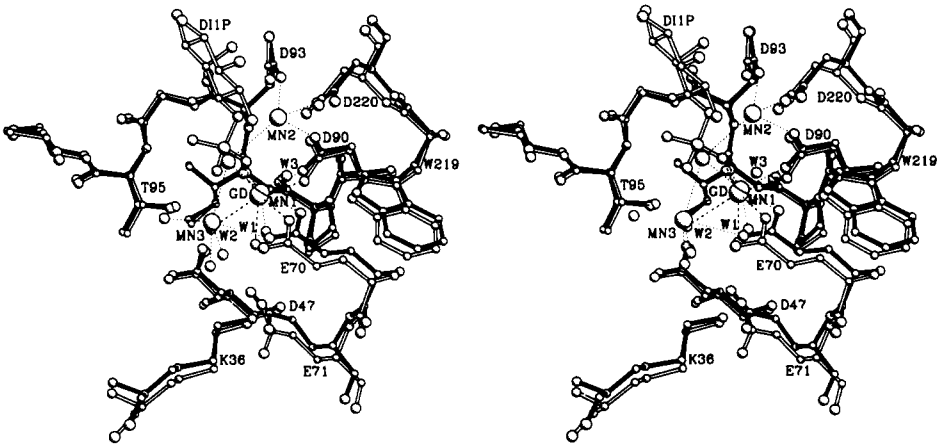

FIGURE 2: Stereodrawing of the superimposed structures of inositol monophosphatase complexes with Mn^{2+} (filled bonds) and D-Ins(1)P (open bonds). C_α atoms on the A subunits of the two structures have been superimposed (rms deviation between C_α positions = 0.37 Å). Coordinate bonds to the Mn^{2+} ions are shown as dotted lines, and coordinate bonds to the Gd^{3+} ion are shown as dashed lines. Water molecules W1 and W2 are common to both structures, W3 is from the D-Ins(1)P complex, and the unlabeled water molecules are from the Mn^{2+} complex.

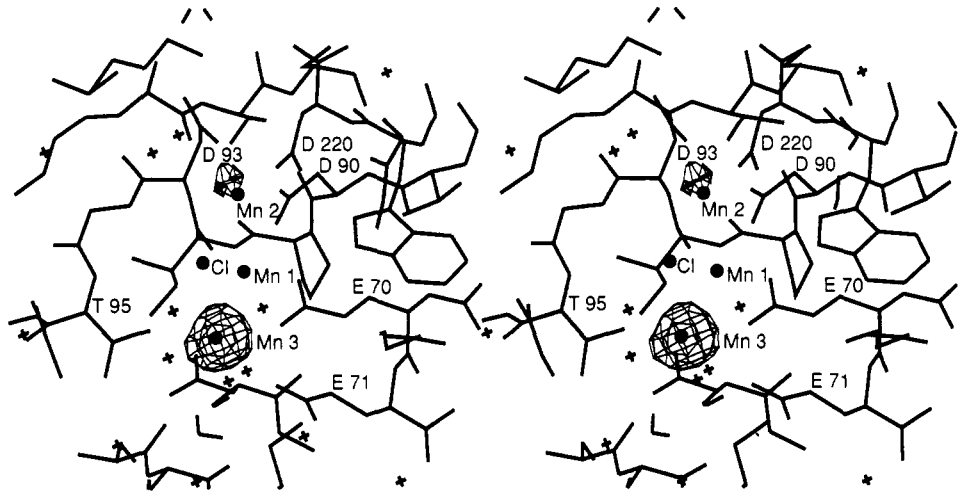

FIGURE 3: Stereodrawing of a difference electron density map of the active site region of the A subunit of the inositol monophosphatase complex with Mn^{2+} and phosphate. The map ($|F_{O1}| - |F_{O2}|$) was made using structure factors from the Mn^{2+} cocrystal (F_{O1}), structure factors from the phosphate-soaked Mn^{2+} cocrystal (F_{O2}), and phases calculated from the final refined model of the Mn^{2+} complex with inositol monophosphatase. The large electron density peak centered on the third metal binding site clearly indicates that Mn^{2+} is present in the Mn^{2+} complex in this site but not in the Mn^{2+} and phosphate complex. The map is contoured at 3 times the rms value of the map. No negative contours were observed at this contour value.

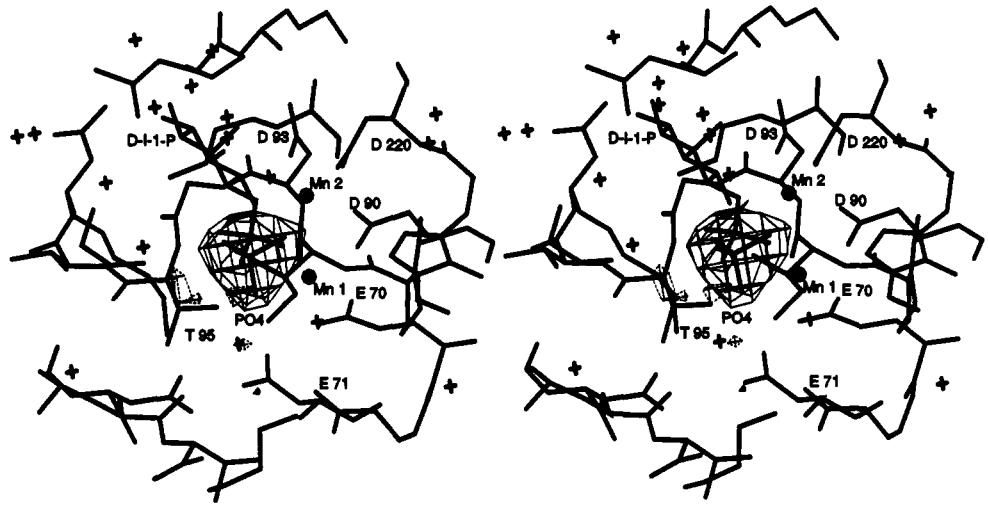

FIGURE 4: Stereodrawing of a difference electron density map ($|F_o| - |F_c|$) of the inositol monophosphatase complex with Mn^{2+} and phosphate. Structure factors (F_c) and phases (ϕ_c) were calculated from the final refined coordinates of the complex minus the coordinates for phosphate. For comparison, coordinates for D-Ins(1)P from the structure of the phosphatase complex with D-Ins(1)P have been superimposed (C_α positions of the A subunits of the structures were superimposed). Crosses represent water molecules and filled circles the metals. Positive contours are displayed as solid lines at 4 times the rms map value, and negative contours are shown as dotted lines at –4 times the rms map value.

The temperature factors for the phosphate molecules (42 Å^2) were higher than those for the Mn^{2+} ions (31 Å^2), suggesting the possibility of some disorder in phosphate binding. The Mn^{2+} ion filling site 3 appears to be replaced by a molecule of solvent which forms hydrogen bonds to both phosphate oxygen O3 and Glu 70 OE1. Values for temperature factors of 42 Å^2 for the phosphate and 16 Å^2 for the water could also be indicative of residual occupancy of the active site by the Mn^{2+} and chloride.

No large structural rearrangements are observed upon phosphate binding. Not surprisingly, the structure is more similar to that of the Mn^{2+} complex than to that of the sulfate or substrate complexes with the rms deviation between superimposed C_α positions of subunit A 0.21 Å for the Mn^{2+} complex and 0.39 Å for both the sulfate complex and the complex with D-Ins(1)P (Bone *et al.*, 1992, preceding paper in this issue). Small adjustments in the structure do occur to accommodate phosphate and changes in the positions of the remaining two metal ions. One conformational adjustment in the phosphate and Mn^{2+} complex relative to the substrate complex involves the movement of residues 70 and 71 to accommodate the displacement of water W2 by the phosphate group. However, OE1 of Glu 70 remains within hydrogen-bonding distance of O3 of the phosphate, suggesting that this oxygen (O3) may be protonated on the enzyme. Another adjustment involves the movement of residues 213–220 in response to the absence of the inositol ring and the ester oxygen of the substrate.

Phosphate is bound to inositol monophosphatase with the phosphate orientation inverted with respect to the binding mode of the phosphate group in substrate complexes with the enzyme (Figures 4 and 5). Atom O3 of the phosphate replaces the metal-bound water molecule (W2), which had been identified as the active site nucleophile on the basis of the structures of substrate complexes with the enzyme (Bone *et al.*, preceding paper in this issue) and the coordinates to the Mn^{2+} ion filling site 1. The other three phosphate oxygens roughly overlap with corresponding oxygens from the phosphate group of the substrate and interact with the enzyme in a similar manner as the substrate. Although some disorder

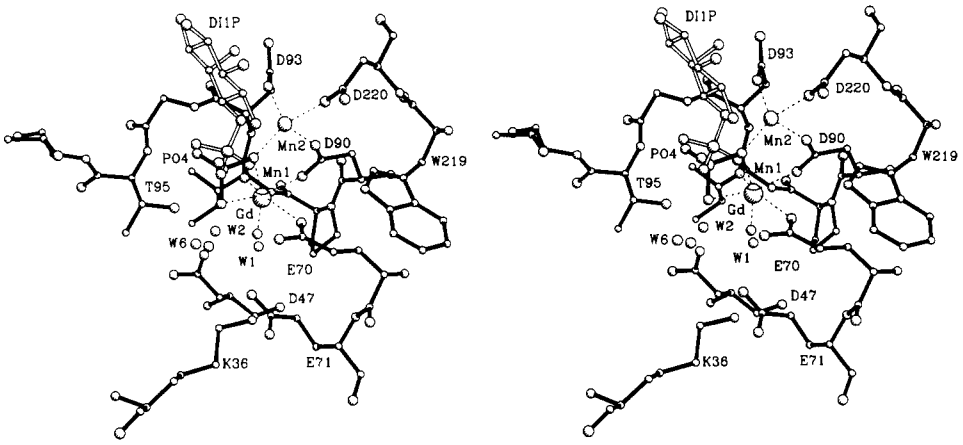

FIGURE 5: Stereodrawing of the active site of the structure of the complex of inositol monophosphatase with Mn^{2+} and phosphate (filled bonds). The structures of the bound substrate, Gd^{3+}, and selected solvent molecules from the structure of the phosphatase complex with D-Ins(1) and Gd^{3+} have been superimposed in open bonds by aligning the C_α atoms of one subunit of the substrate complex with the corresponding atoms of the phosphate complex. Possible coordinate bonds are shown with dashed lines.

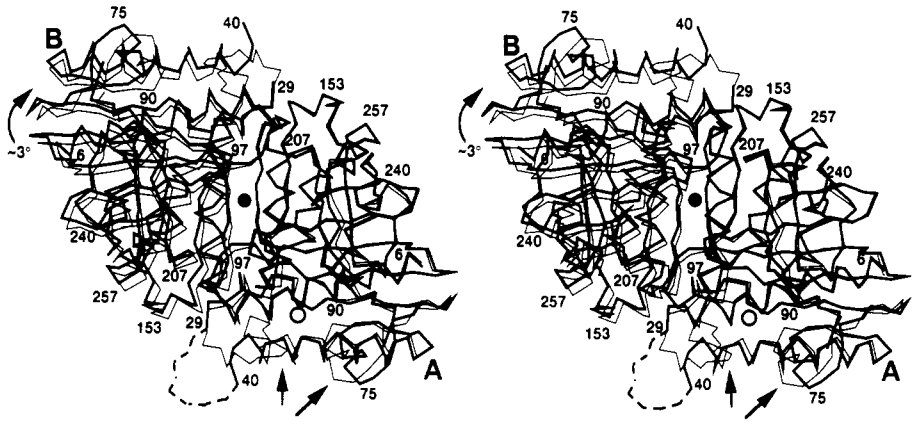

FIGURE 6: Stereodrawing of C_α tracings of the superimposed structures of the apoenzyme (thick lines) and the Gd^{3+} and sulfate-complexed (thin lines) inositol monophosphatase. The C_α atoms of the A subunits of the two structures were superimposed. The B subunit of the apoenzyme was generated by a crystallographic symmetry operation. The relative orientations of the A and B subunits in the apoenzyme have adjusted by rotation of ~3° about the noncrystallographic two-fold axis (filled circle). Residues 29–40 in the apoenzyme are completely disordered and are shown as a dotted line. Arrows identify the residues (residues 29–40 and 70–75 in the Gd^{3+} complex) which undergo the largest conformational change when the metal ions are removed. The approximate location of the Gd^{3+} binding site is shown by the open circle.

may be present in the phosphate position, the electron density is not consistent with the position and orientation of the phosphate group in complexes of substrates and Gd^{3+} with the enzyme (Figure 4).

Conformational Transitions in Mn^{2+} Complexes. The structures of complexes of inositol monophosphatase with divalent cations differ significantly from the complex with Gd^{3+} in the region of the metal binding site which appears to have expanded upon substitution of divalent Mn^{2+} for trivalent Gd^{3+}. The rms deviation between C_α positions in the Gd^{3+} and sulfate and the Mn^{2+} complexes is 0.39 Å when only the A subunits are compared and 0.41 Å if entire dimers are superimposed. The C_α positions of residues 90 and 95, which are on opposite sides of a kink in the protein chain that wraps around the metal binding site, adjust away from each other in a concerted fashion by 1 Å when Gd^{3+} is replaced. In addition, other residues which interact either directly (Glu 70) or indirectly (Glu 71 and Asp 47) with the metal adjust away from the original Gd^{3+} location by up to 0.5 Å. These conformational adjustments are very similar to adjustments which have been observed in the structures of complexes of the enzyme with Gd^{3+} and substrates (Bone *et al.*, preceding paper in this issue).

Apoenzyme Structure. The structure of the apoenzyme retains the secondary structure observed in the phosphatase complex with Gd^{3+} and sulfate but has adjusted to the absence of a metal cation in several ways. Without a metal cofactor, inositol monophosphatase has crystallized in a form in which the asymmetric unit of the crystal is a phosphatase subunit rather than the phosphatase dimer which is observed in the structures of phosphatase complexes with Gd^{3+} or Mn^{2+}. The relative orientations of the two subunits in the phosphatase dimer have adjusted by a rotation of approximately 3° about the dimer two-fold axis so that the axis is now an exact (crystallographic) rather than an approximate two-fold axis (Figure 6). Although the arrangement of secondary structure elements is unchanged in the apoenzyme, several large conformational changes have occurred. In response to the 3° rotation about the noncrystallographic two-fold axis, the two-turn helix comprised of residues 95–100 adjusts away from the metal binding site and into the subunit interface (Figure 7). This conformational change allows residues 100–103 to maintain contact with residues 202–207 on the adjacent subunit of the dimer. In phosphatase complexes with cations, residues 29–46 wrap around the base of the metal binding site and interact with protein and solvent metal ligands. In the absence of metals, residues 29–46 become disordered and appear to extend into a large solvent channel. An adjacent molecule in the crystal occupies the positions filled by residues 35–39 in the Gd^{3+} complex, and this intermolecular contact may be partly responsible for the conformational change.

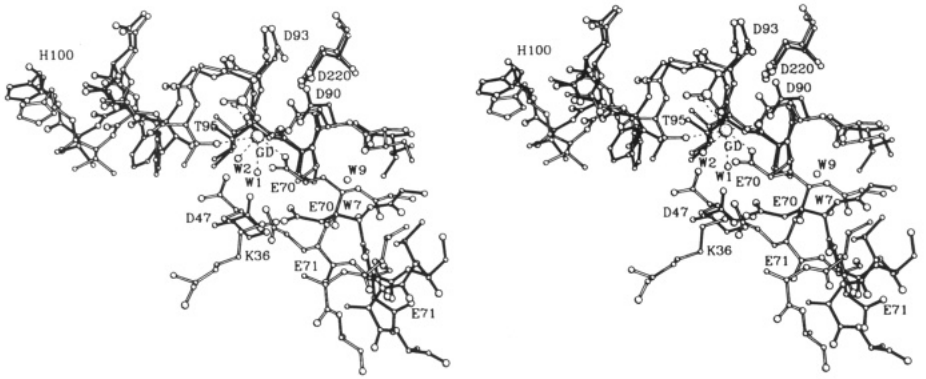

FIGURE 7: Stereodrawing of the superimposed structures (as in Figure 6) of the apoenzyme (filled bonds) and the Gd^{3+} and sulfate-complexed (open bonds) inositol monophosphatase. Coordinate bonds to the Gd^{3+} ion are shown as dashed lines. Large conformational changes have occurred in the region of the metal binding site.

In phosphatase structures in which metal cations are present, residues 70–75 on each subunit form a two-turn α helix containing two Glu residues. Glu 70 is a direct metal ligand, and Glu 71 interacts with one of the metal-bound water molecules (W1). In the absence of metals, this helix adjusts as a rigid body away from the metal binding site by 2–3 Å, breaking three intramolecular hydrogen bonds and creating a gap between the helix and the body of the protein (Figures 6 and 7). The hydrogen-bonding interactions which are lost when the cation is removed are replaced by interactions with two molecules of solvent which form hydrogen bonds that bridge between hydrogen bond donors on the helix and hydrogen bond acceptors on the body of the protein. Residues 90–95 kink around the metal binding site, contribute two ligands to the metal, and interact with one of the metal-bound water molecules. Residues 90 and 95, which are on opposite sides of the metal binding site, move away from each other by 2.6 Å in the absence of metal. Other residues which are involved indirectly in Gd^{3+} binding have also adjusted away from the metal binding site.

Metal binding site 2 is formed from residues Asp 90, Asp 93, and Asp 220, whose carboxylate atoms approach to within 3 Å of each other in substrate and sulfate complexes with the phosphatase in the presence of Gd^{3+} and Li^{+} (Bone *et al.*, 1992, preceding paper in this issue). In the absence of cations, the carboxylate groups of residues 90 and 220 remain within hydrogen-bonding distance of each other (2.89 Å) but have adjusted away from Asp 93 (3.36, 3.50 Å). The pH at which this structure was determined, pH 5.0, would be consistent with either Asp 90 or Asp 220 retaining a proton to allow the formation of a hydrogen bond. However, the observation that Asp 93 adjusts away from the other Asp residues at low pH suggests that the close approach of the three Asp residues in complexes with cations is stabilized by the binding of a metal cation rather than a proton.

DISCUSSION

Mechanism. Structural studies of complexes of inositol monophosphatase with Gd^{3+} and sulfate, D-Ins(1)P, or L-Ins(1)P led to the conclusion that the enzyme catalyzes phosphate ester hydrolysis by promoting the attack of a metal-bound water on the phosphate group of the substrate (Figure 8; Bone *et al.*, 1992, preceding paper in this issue). The metal-coordinated water nucleophile appeared to be activated by hydrogen-bonding interactions with Glu 70 and Thr 95 and would be in line with the leaving group during the transition state. Two mechanisms were proposed to explain how the enzyme facilitates expulsion of the leaving group (Bone *et al.*, preceding paper in this issue). One proposal was that the close proximity of Asp 90, Asp 93, and Asp 220 increases the pK_a value of one of the Asp residues, which retains its proton at neutral pH. Leaving group expulsion would be promoted by donation of the proton from this aspartate to the ester oxygen during the transition state. Alternately, it was proposed that Asp 90, Asp 93, and Asp 220 could form a second Mg^{2+} binding site from which Mg^{2+} would coordinate the ester oxygen and stabilize the development of negative charge as the phosphate ester is cleaved.

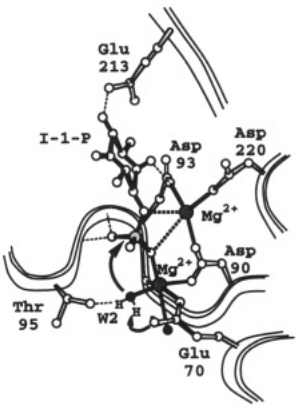

FIGURE 8: Proposed mechanism of action of inositol monophosphatase.

In this work, it has clearly been demonstrated that Asp 90, Asp 93, and Asp 220 form a metal binding site which is capable of binding Mn^{2+}, a divalent cation that supports partial activity (Pollack *et al.*, 1994; Takimoto *et al.*, 1985). Furthermore, in the structure of the apoenzyme, determined at low pH in the absence of metal cations, the three Asp residues move apart. If the close approach of these residues was stabilized by proton binding, the residues would be expected to remain in close proximity at low pH. In addition, metal titration experiments have demonstrated the existence of two kinetically distinct metal-binding environments (Pollack *et al.*, 1994). Finally, Mg^{2+} activation of the enzyme is cooperative with a Hill coefficient of 1.9 (Ganzhorn & Chanal, 1990; Leech *et al.*, 1993), which would be consistent with catalysis using two metal ions. These observations suggest strongly that two metal ions are involved in the mechanism of action of inositol monophosphatase.

Surprisingly, a third Mn^{2+} binding site was observed on each subunit of the phosphatase in Mn^{2+} cocrystals. Is this third metal binding site involved in the catalytic mechanism, or is it an inhibitory site? Displacement of the third metal ion by the addition of phosphate suggests that the third metal

binding site has poor affinity for Mn^{2+} and that only two metal ions are involved in catalysis. In addition, the observation that the third metal binding site has only one direct protein ligand also suggests that it is not involved in catalysis. Because the proposed metal-bound water nucleophile is displaced by the third Mn^{2+} in the phosphatase complex with Mn^{2+} and Cl^-, binding of a metal at the third site might explain the inhibition of inositol monophosphatase observed at high concentrations of activating metals.

On the basis of the inositol monophosphatase structures presented in this work and previous work (Bone *et al.*, 1992, preceding paper in this issue), a composite picture of the transition state can be created. The structures of complexes of inositol monophosphatase with substrates and with phosphate and Mn^{2+} are key elements of the composite which appear to provide snapshots of the reaction pathway on either side of the transition state (Figure 5). Both metal ions appear to participate in substrate and product binding and in stabilization of the trigonal bipyramidal transition state geometry. One metal ion (site 1) has octahedral coordination geometry and stabilizes the development of negative charge on the nucleophilic water. The other metal ion (site 2) has tetrahedral coordination geometry and stabilizes the development of negative charge on the leaving group. The second metal ion may become five coordinate as the transition state is approached. Additional transition state stabilization is provided by interaction of the phosphate group with the amide groups of residues 94 and 95 and through interactions of the inositol group with residues 93, 196, 213, and 220 which may improve during the transition state (Bone *et al.*, preceding paper in this issue).

Studies of nonenzymatic phosphoryl transfer reactions have shown that divalent cations can enhance reaction rates by stabilizing the development of negative charge on the leaving group (Herschlag & Jencks, 1987). In addition, several precedents exist for the use of two metal ions in enzyme-catalyzed phosphoryl transfer reactions. Examples of enzymes that catalyze phosphate ester hydrolysis using two metal ions include alkaline phosphatase (Kim & Wyckoff, 1990), in which catalysis is accomplished by two Zn^{2+} ions, DNA polymerase I (Derbyshire *et al.*, 1988; Freemont *et al.*, 1988), which uses two Mg^{2+} ions, and fructose-1,6-bis(phosphatase) (Zhang *et al.*, 1993a), which uses two Mg^{2+} ions. Fructose-1,6-bis-(phosphatase) is a particularly compelling precedent for two-metal ion catalysis because inositol monophosphatase and the bis(phosphatase) have nearly identical topologies and all of the residues involved in metal binding are conserved (Zhang *et al.*, 1993b). Furthermore, additional kinetic studies of the enzyme (Pollack *et al.*, 1994) suggest strongly that two metal ions are invovled in the mechanism of action of inositol monophosphatase.

Cation Specificity. Structural studies of apoinositol monophosphatase have shown that extensive flexibility is present in the segments of the enzyme which participate in the formation of metal binding sites 1 and 3. Residues 30–40, which interact with both the protein and water ligands of cation binding sites 1 and 3, become completely disordered in the structure of the apoenzyme. Glu 70 and Glu 71, which interact either directly or indirectly with metal binding sites 1 and 3, are part of a two-turn α helix spanning residues 70–75 which moves away from the metal binding site by 2–3 Å when no metals are present. In addition, concerted adjustments of several segments of the structure away from the metal binding sites are observed when the structures of complexes of the enzyme with Mn^{2+} or substrates are compared to the structure of the Gd^{3+} and sulfate complex (Bone *et al.*, 1992, preceding paper in this issue).

Several features of metal binding site 1 of inositol monophosphatase are common to other Mg^{2+} dependent enzymes which exhibit poor cation selectivity. Recent analysis of the structure and metal-binding specificity of one of these enzymes, the phosphorylation-activated signaling protein CheY, has led to the conclusion that poor metal-binding specificity arises when one hemisphere of the cation is coordinated by solvent (Needham *et al.*, 1993). When part of the coordination sphere is provided by solvent, the sphere can be expanded more easily to add extra ligands and the size of the sphere can be increased to accommodate larger ions. Metal binding site 1 of inositol monophosphatase has three enzyme ligands and three solvent or substrate ligands. This binding site appears to have the general features which confer poor metal ion selectivity on many Mg^{2+} dependent enzymes (Needham *et al.*, 1993). These features together with segmental flexibility in many of the residues which form metal binding site 1 explain the poor ion selectivity of the enzyme.

Conclusions. Three metal binding sites have been observed in the active site of inositol monophosphatase using X-ray crystallography. Displacement of one of the three metal ions by phosphate addition suggests that two of the sites are involved in catalysis and the third is an inhibitory site. In the two-metal ion mechanism, one metal activates the nucleophile while the second stabilizes the development of negative charge on the leaving group. Both metals may stabilize the transition state geometry and the charge distribution. The absence of strong enzyme selectivity for Mg^{2+} appears to be derived from flexibility in several segments of the protein which are involved in metal binding and from the presence of several solvent ligands in the coordination spheres of two of the metal binding sites.

ACKNOWLEDGMENT

We thank Dr. D. Herschlag for useful discussions regarding the mechanism of inositol monophosphatase action.

REFERENCES

Berridge, M. J., & Irvine, R. F. (1989) *Nature 341*, 197–205.
Berridge, M. J., Downes, C. P., & Hanley, M. R. (1982) *Biochem. J. 206*, 587–595.
Berridge, M. J., Downes, C. P., & Hanley, M. R. (1989) *Cell 59*, 411–419.
Bone, R., Springer, J. P., & Atack, J. R. (1992) *Proc. Natl. Acad. Sci. U.S.A. 89*, 10031–10035.
Bone, R., Frank, L., Springer, J. P., Pollack, S. J., Osborne, S., Atack, J. R., Knowles, M. R., McAllister, G., Ragan, C. I., Broughton, H. R., Baker, R., & Fletcher, S. R. (1994) *Biochemistry* (preceding paper in this issue).
Browne, K. A., & Bruice, T. C. (1992) *J. Am. Chem. Soc. 114*, 4951–4958.
Brunger, A. T., Kuriyan, J., & Karplus, M. (1987) *Science 235*, 458–460.
Brunger, A. T., Krukowski, A., & Erickson, J. (1990) *Acta Crystallogr. A46*, 585–593.
Carrell, C. J., Carrell, H. L., Erlebacher, J., & Glusker, J. P. (1988) *J. Am. Chem. Soc. 110*, 8651–8656.
Chin, J., Banaszczyk, M., Jubian, V., & Zou, X. (1989) *J. Am. Chem. Soc. 111*, 186–190.
Crowther, R. A. (1972) in *The Molecular Replacement Method* (Rossmann, M. G., Ed.) pp 173–178, Gordon and Breech, New York.
Crowther, R. A., & Blow, D. M. (1967) *Acta Crystallogr.* 23, 544–548.

Derbyshire, V., Freemont, P. S., Sanderson, M. R., Beese, L., Friedman, J. M., Joyce, C. M., & Steitz, T. A. (1988) *Science 240*, 199–201.
De Rosch, M. A., & Trogler, W. C. (1990) *Inorg. Chem. 29*, 2409–2416.
Diehl, R. E., Whiting, P., Potter, J., Gee, N., Ragan, C. I., Linmeyer, D., Schoepfer, R., Bennet, C., & Dixon, R. A. F. (1990) *J. Biol. Chem. 265*, 5946–5949.
Felhammer, H., & Bode, W. (1975) *J. Mol. Biol. 98*, 683–692.
Fife, T. H., & Pujari, M. P. (1988) *J. Am. Chem. Soc. 110*, 7790–7797.
Fitzgerald, P. M. D. (1988) *J. Appl. Crystallogr. 21*, 273–278.
Freemont, P. S., Friedman, J. M., Beese, L. S., Sanderson, M. R., & Steitz, T. A. (1988) *Proc. Natl. Acad. Sci. U.S.A. 85*, 8924–8928.
Ganzhorn, A. J., & Chanal, M.-C. (1990) *Biochemistry 29*, 6065–6071.
Gee, N. S., Ragan, C. I., Watling, K. J., Aspley, S., Jackson, R. G., Reid, G. G., Gani, D., Shute, J. K., *et al.* (1988) *Biochem. J. 249*, 883–889.
Hallcher, L. R., & Sherman, W. R. (1980) *J. Biol. Chem. 255*, 10896–10901.
Hendrickson, W. A. (1985) *Methods Enzymol. 115*, 252–271.
Herschlag, D., & Jencks, W. P. (1987) *J. Am. Chem. Soc. 109*, 4665–4674.
Howard, A. J., Gilliland, G. L., Finzel, B. C., Poulos, T. L., Ohlendorf, D. H., & Selemme, F. R. (1987) *Acta Crystallogr. 20*, 383–387.
Huheey, J. E. (1978) *Inorganic Chemistry*, 2nd ed., Harper, New York.
Jones, D. R., Lindoy, L. F., & Sargeson, A. M. (1983) *J. Am. Chem. Soc. 105*, 7327–7336.
Jones, T. A. (1978) *J. Appl. Crystallogr. 11*, 268–272.
Kim, E. E., & Wyckoff, H. W. (1991) *J. Mol. Biol. 218*, 449–464.
Leech, A. P., Baker, G. R., Shute, J. K., Cohen, M. A., & Gani, D. (1993) *Eur. J. Biochem. 212*, 693–704.
Majerus, P. W., Connoly, T. M., Bansal, V. S., Inhorn, R. C., Ross, T. S., & Lips, D. L. (1988) *J. Biol. Chem. 263*, 3051–3054.
Mathews, B. W. (1968) *J. Mol. Biol. 33*, 491–496.
McAllister, G., Whiting, P., Hammond, E. A., Knowles, M. R., Atack, J. R., Bailey, F. J., Maigetter, R., Ragan, C. I., *et al.* (1992) *Biochem. J. 284*, 749–754.
Needham, J. V., Chen, T. Y., & Falke, J. J. (1993) *Biochemistry 32*, 3363–3367.
Pollack, S. J., Knowles, M. R., Atack, J. R., Broughton, H. B., Ragan, C. I., Osborne, S. A., & McAllister, G. (1993) *Eur. J. Biochem. 217*, 281–287.
Pollack, S. J., Jackson, R. G., Atack, J. R., Knowles, M. R., McAllister, G., Ragan, C. I., Broughton, H. B., Baker, R., & Fletcher, S. R. (1994) *Proc. Natl. Acad. Sci. U.S.A.* (in press).
Sack, J. S. (1988) *J. Mol. Graphics 6*, 224–225.
Sherman, W. R., Gish, B. G., Honchar, M. P., & Munsell, L. Y. (1986) *Fed. Proc. 45*, 2639–2646.
Sussman, J. L. (1985) *Methods Enzymol. 115*, 271–303.
Takimoto, K., Okada, M., Matsuda, Y., & Nakagawa, H. (1985) *J. Biochem. 98*, 363–370.
Ward, K. B., Wishner, B. C., Lattman, E. E., & Love, W. E. (1975) *J. Mol. Biol. 98*, 161–177.
Zhang, Y., Liang, J.-Y., Huang, S., Ke, H., & Lipscomb, W. N. (1993a) *Biochemistry 32*, 1844–1857.
Zhang, Y., Liang, J.-Y., & Lipscomb, W. N. (1993b) *Biochem. Biophys. Res. Commun. 190*, 1080–1083.